# Seasonal patterns of tropical forest leaf area index and $CO_2$ exchange

Christopher E. Doughty[1] and Michael L. Goulden[1]

Received 12 September 2007; revised 16 June 2008; accepted 24 July 2008; published 14 October 2008.

[1] We used in situ and satellite measurements to investigate the seasonal patterns of leaf area index (LAI) and gross ecosystem $CO_2$ exchange (GEE) by an evergreen tropical forest. The forest experienced a dry season from June through November. The rates of light-saturated $CO_2$ uptake (GEE) were comparatively high from December through March and low from May through July. In situ measurements showed that LAI varied seasonally, with a minimum from May through September. Leaf production and leaf abscission were reduced from December through April. Leaf abscission increased in May, which reduced LAI. High rates of leaf abscission and production occurred from July through September associated with leaf turnover. Leaf abscission decreased abruptly in October, while production continued, which rapidly increased LAI. Leaf phenology was not directly correlated with changes in soil water. The seasonal cycle of in situ LAI differed markedly from the seasonal cycles of in situ normalized difference vegetation index (NDVI) and the Moderate Resolution Imaging Spectroradiometer (MODIS) MOD15 LAI product. We hypothesize that the NDVI and MOD15 seasonality at the site is driven partly by seasonal changes in leaf age and leaf reflectance. We developed three simple models to investigate the causes of GEE seasonality. The first two models showed that the seasonal changes in LAI alone, and the effects of leaf age on leaf-level photosynthesis alone, could not account for the observed GEE seasonality. The third model showed that the combined effect of seasonal changes in LAI and seasonal changes in leaf age and leaf photosynthesis was sufficient to account for the observed GEE seasonality.

**Citation:** Doughty, C. E., and M. L. Goulden (2008), Seasonal patterns of tropical forest leaf area index and $CO_2$ exchange, *J. Geophys. Res.*, *113*, G00B06, doi:10.1029/2007JG000590.

## 1. Introduction

[2] Many tropical forests, including those in the eastern Amazon basin, experience extended dry seasons. Early researchers [*Malhi et al.*, 1998] and models [*Williams et al.*, 1998] indicated that evergreen tropical forest photosynthesis declines during the dry season with drought stress. More recent studies within the Large-Scale Biosphere-Atmosphere Experiment in Amazonia (LBA-ECO) have found that evergreen tropical forests often avoid drought stress [*Saleska et al.*, 2003], and that the photosynthetic capacity of some forests actually increases before the end of the dry season. For example, *Goulden et al.* [2004] reported that the light-saturated rate of canopy photosynthesis at the LBA-ECO Tapajós km-83 evergreen forest, which experiences a dry season from ~July through ~December, was ~30% greater from October to April than from May to September.

[3] The ability of tropical trees to avoid drought stress is almost certainly related to deep rooting and access to sufficient soil water [*Nepstad et al.*, 1994; *da Rocha et al.*, 2004; *Bruno et al.*, 2006]. The cause of the late season increase in photosynthetic capacity is less well understood. The two most likely causes are seasonal changes in leaf area index (LAI) and seasonal changes in leaf age and concomitant changes in leaf photosynthesis. *Goulden et al.* [2004] focused on the first possibility and hypothesized that LAI is increased from October to April and that this seasonal increase in LAI is large enough to cause the seasonal increase in $CO_2$ uptake. Based on indirect observations, Goulden et al. suggested the following time line. April: leaf abscission begins, which decreases LAI and canopy photosynthesis. May through September: the population of leaves turns over, which results in an extended period with reduced LAI and canopy photosynthesis. October: leaf abscission ends and leaf growth continues, which increases LAI and canopy photosynthesis. November through March: leaf abscission and growth are reduced, which results in sustained high LAI and canopy photosynthesis.

[4] Quantitative, in situ observations of tropical forest leaf phenology are scarce, though some of the reports available are broadly consistent with Goulden et al.'s hypothesis. Several studies have found that tropical forest litterfall and leaf production peak in the dry season [*van Schaik et al.*, 1993]. Moreover, the enhanced vegetation index (EVI) near km-83 increases in the dry season coincident with increasing $CO_2$ uptake, implying a

[1]Department of Earth System Science, University of California, Irvine, California, USA.


0148-0227/08/2007JG000590

change in leaf growth [*Xiao et al.*, 2005; *Huete et al.*, 2006]. In situ measurements near km-83 showed that LAI peaked at ~6.3 $m^2m^{-2}$ in October and January and declined to ~5.8 $m^2m^{-2}$ in July and August [*Asner et al.*, 2004]. On the other hand, satellite observations of LAI for the Amazon basin differ from Goulden et al.'s hypothesis. *Myneni et al.* [2007] found that the Moderate Resolution Imaging Spectroradiometer LAI Product (the MODIS MOD15 product) is greater from July through October and less from December through May, a pattern that is nearly opposite the cycle hypothesized by *Goulden et al.* [2004].

[5] We used in situ measurements of leaf and canopy gas exchange; leaf abscission, flushing and area; and satellite and in situ measurements of canopy reflectance to investigate the seasonal patterns of LAI and photosynthesis at the km-83 field site. We focused on two questions: (1) How does LAI vary seasonally at km-83? (2) What controls the seasonal changes in whole-forest photosynthesis at km-83? We addressed the first question by developing a new data set of the leaf phenology at km-83. We addressed the second question with a series of simple models that distinguished between the possibility that seasonal change in LAI is the main driver of seasonal change in $CO_2$ uptake, and the alternative possibility that leaf aging is the main driver of seasonal changes in $CO_2$ uptake.

## 2. Methods

### 2.1. Site

[6] This study was conducted at the LBA-ECO km-83 site (−3.020833 S, 54.972221W) in the Floresta National do Tapajós (FLONA). The FLONA Tapajós extended from 50- to 150-km south of Santarém, Para, Brazil, on the eastern side of the Tapajós River. The vegetation was closed tropical forest, with a canopy height of ~40 m and scattered emergent trees up to 55 m. The FLONA was in the 27th percentile (±2 to 3%) of Amazonian forests with respect to both annual precipitation and wet season length [*Saleska et al.*, 2003]. The forest was on a broad, flat plateau [*Goulden et al.*, 2006]. Soils were mainly yellow latosol clay (Haplic acrorthox).

[7] An area extending 2- to 3-km east of the main km-83 eddy covariance tower was selectively logged in September 2001 as part of the larger LBA-ECO experiment. The logging was patchy, creating a mosaic of new gaps within patches of relatively intact forest. The logging removed ~12% of the large trees and increased the area of gaps from ~4% to ~12% [*Miller et al.*, 2007; *Figueira et al.*, 2008]. The rates and seasonality of $CO_2$ exchange and the stem increment by large trees were largely unchanged by the logging [*Figueira et al.*, 2008]. The stem increment by smaller, understory trees [*Figueira et al.*, 2008] and the ventilation of the subcanopy [*Miller et al.*, 2007] were increased following logging. The changes in subcanopy ventilation and small-tree growth imply that the logging opened the canopy and increased the amount of light reaching the understory, even in areas that were not immediately adjacent to gaps [*Figueira et al.*, 2008].

### 2.2. Tower Measurements

[8] We used the eddy covariance method [*Baldocchi*, 2003; *Wofsy et al.*, 1993] to measure the turbulent fluxes of $CO_2$, sensible heat, latent heat, and momentum at 64-m above ground level [*Goulden et al.*, 2004; *da Rocha et al.*, 2004; *Miller et al.*, 2004]. The eddy covariance measurements began in late June 2000 and ended in March 2004, when a large tree fall destroyed the tower. The wind and temperature were recorded at 4 Hz with a 3-dimension sonic anemometer (Campbell Scientific, Logan, UT). The $CO_2$ and $H_2O$ densities were measured with a Li-Cor 7500 open path infrared gas analyzer (IRGA) (Li-Cor Biosciences, Lincoln, NE). We made density corrections to the open path IRGA measurements following *Miller et al.* [2004]. We mathematically rotated the wind so that both the mean cross and vertical components averaged zero over each half hour period [*Miller et al.*, 2004]. We simultaneously measured the change in $CO_2$ stored between the ground and 64 m by sequentially sampling the $CO_2$ mixing ratio at 12 altitudes using a manifold of solenoid valves and a closed-path IRGA (Li-Cor Biosciences). We calculated the half-hour net ecosystem $CO_2$ exchange (NEE) as the sum of the eddy and storage fluxes.

[9] We calculated the forest's gross ecosystem exchange (GEE) from the observations of NEE by subtracting the rates of whole-forest respiration observed at night [*Goulden et al.*, 2006]. We calculated respiration at three-day intervals by averaging the NEE observed during nocturnal periods. Our analysis of GEE focused on the rates of light saturated $CO_2$ uptake, which we defined as observations with an incident short-wave irradiance greater than 700 $Wm^{-2}$ [*Goulden et al.*, 2004].

[10] All meteorological measurements, including the radiation fluxes, were recorded at 0.5 Hz. Precipitation was measured with a tipping-bucket rain gauge (Texas Electronics TE525, Dallas, Texas, USA). Incoming and reflected photosynthetic photon flux density (PPFD) at 64 m were measured with silicon quantum sensors (LI-COR LI190, Lincoln NE). Incoming and reflected solar radiation at 64 m were measured with thermopile pyranometers (Kipp & Zonen CM6, Delft, The Netherlands). Below-canopy PPDF was measured with 8 quantum sensors (Apogee Instruments, Logan UT) that were horizontally mounted at ~30 cm above the forest floor. The sensors were arrayed at 5-m intervals along two 20-m transects in a forest patch that was ~20 to ~40 m from the nearest logging-created gap and that was ~40 m from the tower.

### 2.3. Leaf Area Index

[11] We determined the seasonal changes in LAI from August 2001 to March 2004 by comparing the continuous measurements of above- and below-canopy PPFD [*Fuchs et al.*, 1984; *Pierce and Running*, 1988; *Welles and Cohen*, 1996; *Bonan*, 2002; *Breda*, 2003; *Wang et al.*, 2004]. We calculated LAI using a simple radiation transfer model:

$$I(z) = I_o e^{-KL(z)}$$

where $I_o$ is the incident PPFD above the canopy, I(z) is the PPFD at height z, L(z) is the cumulative leaf area index between the PPFD sensors, and K is the light extinction coefficient. We set K to 0.5/cos(zenith angle) [*Fuchs et al.*, 1984]. We controlled for the effect of solar angle by considering only observations with zenith angles of 0 to 30°. We controlled for the effect of diffuse radiation by

considering only brightly illuminated periods with an incoming PPFD of 1400 $\mu$mol $m^{-2}$ $s^{-1}$ or greater. We used sensitivity analyses to confirm that our results were independent of both the selection of K and the range of zenith angles. We found that the seasonal patterns of LAI remained constant regardless of K and the accepted range of zenith angles (figures not shown).

[12] Our calculated LAI values increased from $\sim$6 $m^2$ $m^{-2}$ in August 2001 to $\sim$10 $m^2$ $m^{-2}$ in March 2004 (figure not shown). This trend is likely an effect of forest regrowth following logging or of a downward drift in the signals from the below-canopy PPFD sensors associated with aging or the accumulation of dirt on the instrument surfaces. Our focus was on the seasonal patterns of LAI, which showed a similar seasonal pattern throughout the study. We therefore removed the apparent long-term LAI trend.

[13] The main assumptions in using canopy light interception to determine relative seasonal changes in LAI are: (1) the leaf-level light transmittance remains constant year-round, (2) leaf exposure, clumping and tip angle remain constant, (3) solar angle is controlled for, (4) the ratio of diffuse to direct beam light remains constant, and (5) the below-canopy sensors provide a spatial average of below-canopy PPFD. We minimized the effect of seasonal changes in leaf transmittance by focusing on the interception of PPFD rather than total solar radiation [*Roberts et al.*, 1998]. We have no reason to suspect that leaf exposure, clumping or tip angle change seasonally, though we cannot exclude this possibility. We controlled for the effect of solar angle by considering only observations within a specified range of zenith angles. We controlled for the ratio of diffuse to direct beam light by considering only sunny periods with a specified zenith angle. We increased the spatial sampling of below-canopy PPFD by deploying the sensors along two 20-m transects that were at right angles. We feel the 5th source of uncertainty (spatial heterogeneity) presents the greatest risk for our analysis. We therefore quantified this uncertainty by calculating the LAI separately for each sensor and using the variability between sensors to estimate the uncertainty associated with spatial heterogeneity.

### 2.4. Leaf Flush and Abscission

[14] The seasonal pattern of leaf flush was calculated from observations of litterfall and the seasonal changes in LAI. Litter was collected biweekly from 30 1-$m^2$ traps, which were arrayed along two transects to the east of the eddy covariance tower [*Goulden et al.*, 2004]. The litterfall was summed to monthly intervals, and the simultaneous change in LAI was calculated as the derivative of the light-interception measurements (dLAI). Leaf flush was then calculated as the sum of litterfall and dLAI.

### 2.5. Tower-Based Albedos and Vegetation Indices

[15] We calculated several tower-based measures of canopy reflectance, including the visible and near infrared radiation (NIR) albedos and the broadband normalized difference vegetation index ($NDVI_{tower}$) from August 2001 to August 2003. The pyranometers were sensitive to wavelengths from 310 to 2800 nm and the PPFD sensors were sensitive to wavelengths from 400 and 700 nm. We converted PPFD from $\mu$mol $m^{-2}$ $s^{-1}$ to W $m^{-2}$ by multiplying by 0.25 J $\mu mol^{-1}$, based on the energy of photons in green light [*Huemmrich et al.*, 1999]. We calculated the flux of energy in the NIR as the difference between the pyranometer and quantum sensor observations.

[16] We calculated the visible albedo ($PPFD_A$) by dividing the reflected PPFD ($PPFD_{up}$) by the incident PPFD ($PPFD_{down}$). We calculated the total solar albedo by dividing the reflected solar energy (pyranometer $_{up}$) by the incident solar energy (pyranometer $_{down}$). We calculated the NIR albedo ($NIR_A$) by dividing the reflected NIR ($NIR_{up}$) by the incident ($NIR_{down}$). We calculated $NDVI_{tower}$ as:

$$NDVI_{tower} = (NIR_A - PPFD_A)/(NIR_A + PPFD_A).$$

$NDVI_{tower}$ has been found to correlate well with narrow-band NDVI [*Huemmrich et al.*, 1999], and to be largely insensitive to seasonal changes in solar zenith angle. The $NDVI_{tower}$ for the entire year at km-83 changed from 0.76 to 0.81 over the course of the day with zenith angle (figure not shown).

### 2.6. Leaf Gas Exchange

[17] We measured the leaf-level gas exchange off scaffold towers [*Doughty et al.*, 2006; *Doughty and Goulden*, 2008] at the LBA-ECO km-83 [*Goulden et al.*, 2004], km-67 [*Saleska et al.*, 2003], and Seca Floresta [*Nepstad et al.*, 2002] field sites. All of the sites were in closed-canopy evergreen forest in the FLONA Tapajós. The km-83 scaffold was located within 300 m of the main eddy flux tower.

[18] We used a portable gas exchange system (LI 6400, Li-Cor Biosciences, Lincoln, NE) at the km-83 site from August to December 2004 and at all of the sites from August to January 2005. We measured the rates of gas exchange under a standardized set of conditions (temperature 30°C; PPFD 1000 $\mu$mol $m^{-2}$ $s^{-1}$; ambient $CO_2$). We repeatedly measured two leaves on each of two branches for canopy species, and returned to a leaf until it abscised, at which point we choose another nearby leaf.

### 2.7. MODIS Observations for km-83

[19] We processed the MODIS LAI (MOD15A2 V004) observations for km-83 to a monthly time resolution and 8-km spatial resolution following *Myneni et al.* [2007]. We obtained MODIS data from the EOS data gateway (http://edcdaac.usgs.gov/dataproducts.asp). We removed all observations that were either cloud contaminated or that used the empirical retrieval algorithm. We used the MODIS tile calculator to locate the tower (tile 12–9, line 362, sample 612). We centered the 8-km by 8-km square 2 km to the west of the main km-83 tower. The 8-km by 8-km area was located in a block of homogenous forest that was 13 km east to west and 20 km north to south [*Goulden et al.*, 2006]. Finally, we digitized Figure 1A from *Myneni et al.* [2007] and averaged across years to compare the seasonal patterns of MODIS-derived LAI observed at km-83 with those reported for the broader Amazon Basin.

[20] We compared the MODIS-derived black sky broadband NIR (0.7 to 5 $\mu$m) and broadband visible (0.3 to 0.7 $\mu$m) albedos with the tower-based albedos. We obtained MOD43B3 V004 images at 16-day temporal, 8-km spatial resolution from the EOS data gateway website (http://edcdaac.usgs.gov/dataproducts.asp) for April 2002 to March 2003.

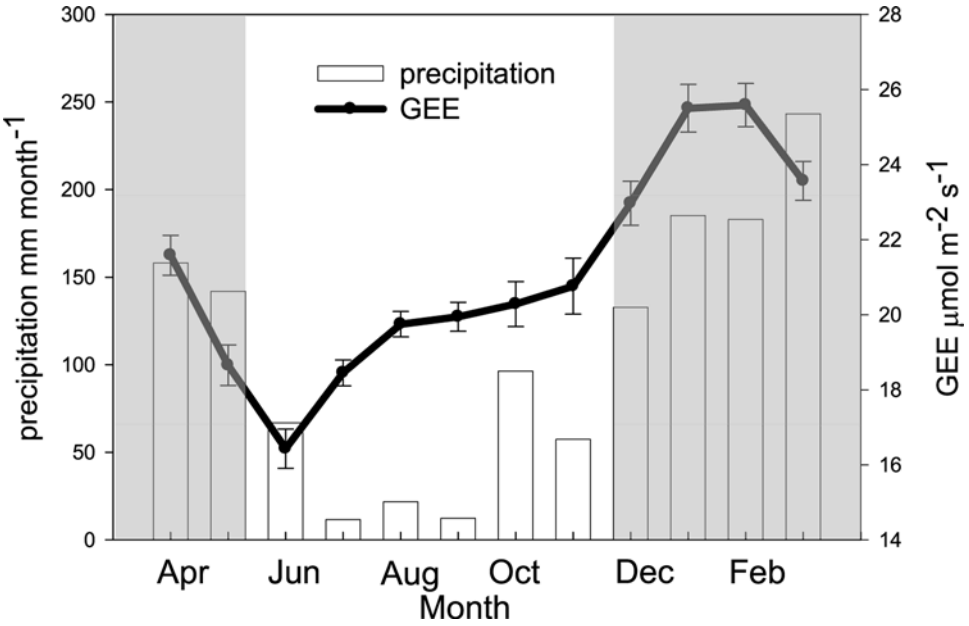


**Figure 1.** Monthly precipitation (open bars; mm month$^{-1}$) and gross ecosystem $CO_2$ exchange (GEE; $\mu$mol m$^{-2}$ s$^{-1}$; solid line connecting monthly averages ± se, n varies from 83 to 320) during sunny periods (incoming shortwave radiation greater 700 W m$^{-2}$) from August 2001 to August 2003 at the LBA-ECO km-83 site. The GEE was calculated from eddy covariance observations of net ecosystem $CO_2$ exchange after accounting for respiration using nocturnal observations. Shaded areas show the typical wet season (months with greater than 100 mm of precipitation).

### 2.8. Leaf Spectral Reflectance Model

[21] We combined the calculated leaf flush data from our site with data on the change in leaf-level NIR absorbance due to epiphylls from *Roberts et al.* [1998] to create a simple model of the seasonal changes in mean leaf-level NIR spectral absorbance. *Roberts et al.* [1998] followed a cohort of leaves from three Amazonian species that flushed in July and August. They placed the leaves into one of four categories (uncolonized by epiphylls, slight colonization, moderate colonization, and necrotic) and measured the NIR absorption for each category. ~70 days after leaf flush the average NIR absorbance for all leaves increased by 0.048. After this initial large increase, the NIR spectral absorbance increased linearly by ~0.0027 month$^{-1}$. We assumed the NIR spectral absorbance of leaves at our site showed similar NIR spectral properties to those measured in by Roberts et al. We quantified our leaf-level NIR albedo as follows: (1) $\Delta$ leaf-level NIR absorbance = % old leaves *average NIR absorbance of 12 month old leaves + % new leaves * NIR absorbance of leaves based on their age and the following 2 equations; (2) If leaf age $\leq$ 2 months then the $\Delta$ NIR absorbance = 0; (3) If leaf age > 2 months then $\Delta$ NIR absorbance = 0.048 + 0.0027 * (months since leaf flush – 3). We then combined the resulting leaf-level albedos and the observed LAI using a two-stream radiation transfer model to calculate whole-canopy NIR albedo [*Dickinson*, 1983].

### 2.9. GEE Models

[22] We used three simple, observation-driven models of canopy gas exchange to investigate the controls on canopy gas exchange seasonality. Each model calculated a single value of canopy photosynthesis under light saturated conditions for each month of the year. The first model assumed that the seasonal shifts in canopy gas exchange were driven solely by seasonal changes in LAI. The second model assumed that seasonal shifts in canopy gas exchange were driven solely by seasonal changes in leaf age and leaf-level photosynthesis. The third model assumed that seasonal shifts in canopy gas exchange were driven by the combination of seasonal changes in LAI and leaf-level photosynthesis. Our focus was on the relative patterns of canopy gas exchange over the year, and we therefore normalized the rates of $CO_2$ uptake by the month with the highest uptake.

[23] The LAI-driven model was based on the observed seasonal changes in LAI. The model calculated canopy photosynthesis as the sum of the rates of gas exchange by sunlit leaves, which were assigned a leaf-level rate of 10 $\mu$mol m$^{-2}$ s$^{-1}$, and shaded leaves, which were assigned a leaf-level rate of 3 $\mu$mol m$^{-2}$ s$^{-1}$, based on observations over the study [see also *Doughty et al.*, 2006; *Doughty and Goulden*, 2008]. The model did not allow the leaf-level rates of gas exchange to vary seasonally. The LAI-driven model calculated the sunlit fraction of leaf area as [*Bonan*, 2002]:

$$L_{sun} = \left(1 - e^{-KL}\right)/K$$

where K is the light extinction coefficient, L is the leaf area index, and $L_{sun}$ is the sunlit leaf fraction. The model assumed a random distribution of leaves, and calculated K as:

$$K = 0.5/\cos(Z)$$

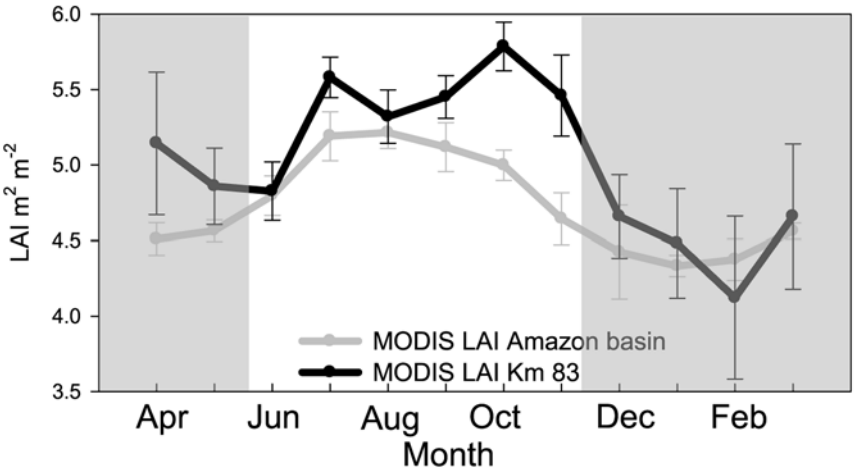


**Figure 2.** Monthly MODIS LAI (MOD15 V004) for the km-83 site (black line connecting monthly averages across years ± sd across years for 2000 to 2006) and monthly MODIS LAI (MOD15 V004) for the Amazon Basin from *Myneni et al.* [2007] (gray line connecting monthly averages ± sd across years for 2000 to 2005). The km-83 observations are for an 8-km by 8-km patch of forest that was centered 2-km west of the km-83 eddy covariance tower. Shaded areas show the typical wet season at km-83.

where Z is the solar zenith angle which we set to 30° [*Bonan*, 2002].

[24] The leaf-age-driven model was based on the reduction in leaf gas exchange that was observed with aging and the rates of leaf turnover that were observed seasonally. The model did not differentiate between sunlit and shaded leaves, and did not allow the LAI to vary seasonally. Rather, the model was driven entirely by the seasonal changes in the proportion of leaves in three age classes: newly flushed leaves, middle-aged leaves, and old leaves. The model set the photosynthetic rate of newly flushed leaves to 2.5 $\mu$mol $m^{-2}$ $s^{-1}$, middle-aged leaves to 5 $\mu$mol $m^{-2}$ $s^{-1}$, and old leaves to 3.75 $\mu$mol $m^{-2}$ $s^{-1}$, based on observations over the study [see also *Doughty et al.*, 2006; *Doughty and Goulden*, 2008]. The rates of leaf flushing and abscission were determined by the flushing and litterfall observations. Leaves remained in the newly flushed class for one month. Leaves transitioned from the middle-aged to the old class at a rate of 20% per month from February to June. The third model was a simple combination of the first two.

## 3. Results

### 3.1. Seasonal Patterns of Canopy $CO_2$ Exchange

[25] The light saturated rates of gross $CO_2$ uptake (GEE) varied seasonally, with comparatively high rates of canopy photosynthesis from December through March and comparatively low rates from May through July (Figure 1). The rates of uptake during the peak months were 30 to 40% greater than the rates during the low months. The seasonal cycle of light-saturated photosynthesis preceded the seasonal cycle of precipitation by one to two months. Light-saturated photosynthesis was greatest in January and February, which was 1 to 2 months before the peak rainfall; photosynthesis was lowest from May through July, which was at the end of the wet season and beginning of the dry season. The amplitude and timing of seasonal patterns of GEE are consistent with those reported for NEE at km-83 during 2000 and 2001 [*Goulden et al.*, 2004].

### 3.2. MODIS LAI

[26] The MODIS LAI product for km-83 showed strong seasonality, with a comparatively high LAI from July through November and a low LAI from December through March (Figure 2). The seasonality, amplitude and magnitude of the LAI observed at km-83 were similar to those reported by *Myneni et al.* [2007] for the entire Amazon Basin. The apparent month-to-month variation in MODIS LAI was greater for km-83 than for the entire Amazon Basin, a difference that almost certainly reflects the much smaller sample size used at km-83.

### 3.3. Seasonal Patterns of Canopy Reflectance

[27] The total short-wave albedo increased over the dry season and decreased during the wet season with an amplitude of 0.02 (Figure 3). This seasonal trend and amplitude are consistent with previous studies [*Carswell et al.*, 2002; *Malhi et al.*, 1998]. The seasonal trend in total albedo was almost entirely a result of seasonal shifts in NIR reflectance. The forest was comparatively dark in the visible (PPFD) and bright in the NIR. The seasonal amplitude of NIR reflectance was 50 times greater than the seasonal amplitude of visible reflectance. The visible albedo varied seasonally by ~0.001, whereas the NIR albedo varied by ~0.05. The seasonal shifts in NIR and PPFD albedo observed by the in situ instruments on the tower were similar to the seasonal trends in NIR and visible albedo observed for km-83 by MODIS.

### 3.4. Tower-Based NDVI and MODIS LAI

[28] The broadband NDVI calculated from the in situ upwelling PPFD and NIR instruments peaked from July to November and declined from January to April (Figure 4). The seasonal pattern of in situ NDVI was very similar to the seasonal pattern of NIR albedo (Figure 3). This similarity is

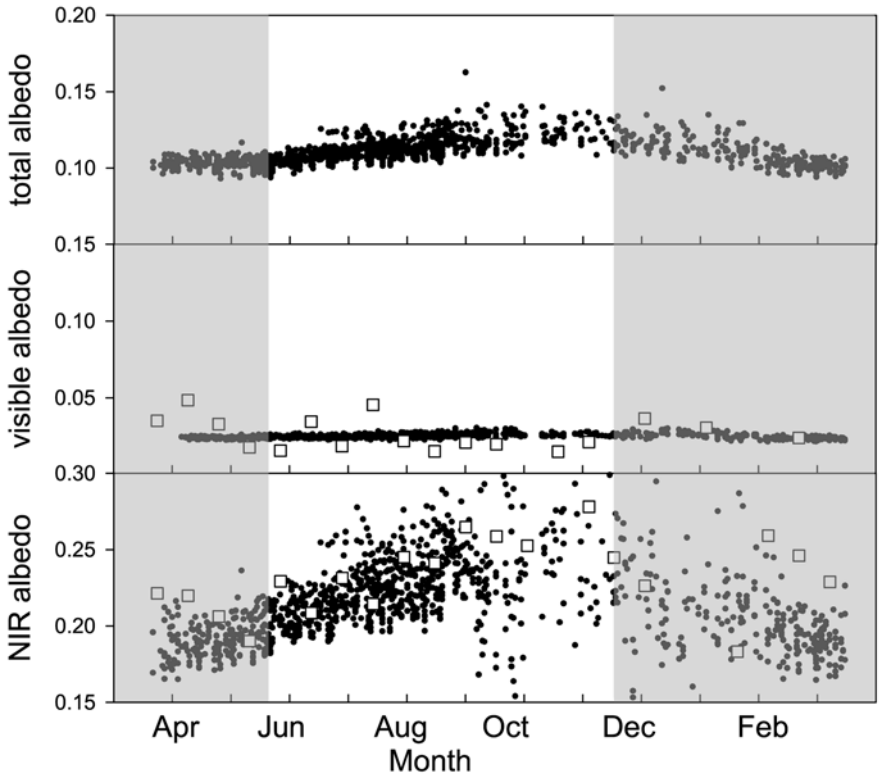


**Figure 3.** (top) Shortwave albedo (a dimensionless ratio calculated by dividing in situ reflected shortwave radiation by incident shortwave radiation) during sunny periods (incoming shortwave radiation greater than 700 W $m^{-2}$). (middle) Visible albedo (calculated by dividing reflected photosynthetic photon flux density (PPFD) by incident PPFD) during sunny periods. (bottom) Near Infrared (NIR) albedo (calculated by dividing reflected NIR by incident NIR) during sunny periods. Black dots in all panels are in situ measurements. Open squares in the lower two panels are 16-day, 8-km MODIS albedos (MOD43B3 black sky) for an area centered 2-km west of the km-83 eddy flux tower. All measurements are for April 2002 to March 2003. Shaded areas show the typical wet season.

expected given the relative seasonal amplitudes of the NIR and visible albedos, and underscores the importance of understanding the seasonal changes in NIR reflectance for efforts to apply optical remote sensing methods at km-83.

[29] The seasonal pattern of in situ NDVI was very similar to the MODIS LAI for the site (Figure 4). Both MODIS LAI and in situ NDVI were increased from July through November and decreased during January and February. The MODIS LAI product was somewhat more variable from month-to-month than the in situ NDVI. The increased variability for the MODIS product may reflect the difficulty of obtaining truly cloud-free pixels from space-borne instruments during the tropical wet season [*Cohen et al.*, 2006]. The similarity between the in situ measurements of reflectance and the MODIS LAI product implies that the seasonal cycle of MODIS LAI is largely a consequence of the large increase in NIR reflectance during the middle and late dry season (Figure 3).

### 3.5. In Situ LAI

[30] We used continuous, in situ measurements of the amount of light intercepted by the canopy to calculate the seasonal patterns of LAI. This approach is especially appropriate for determining the relative seasonal changes in LAI [*Breda*, 2003; *Wang et al.*, 2004]. LAI calculated using the light interception method is relatively insensitive to changes in the spectral reflectance of leaves, and it provides a measure of LAI that is largely independent of ones derived using spectral reflectance.

[31] The LAI calculated from light interception varied seasonally, reaching a minimum from May through September and a maximum from October through April (Figure 4). The seasonal pattern of LAI derived from light interception is very similar to that inferred by *Goulden et al.* [2004], and is generally in phase with the rates of canopy photosynthesis observed at the site (Figure 1). On the other hand, the seasonal cycle of LAI calculated from light interception differs markedly from the seasonal cycles of in situ NDVI and MODIS LAI (Figure 4).

### 3.6. Leaf Phenology

[32] We combined the seasonal changes in in situ LAI with litterfall collections to calculate the patterns of leaf production (Figure 5). Litterfall was comparatively low from November through April and high from May through September. Literfall peaked in August and September. The derivative of LAI (dLAI) remained around zero from November though March, implying that the LAI was constant during this period. dLAI was strongly negative in April and May, implying a reduction in LAI. dLAI was

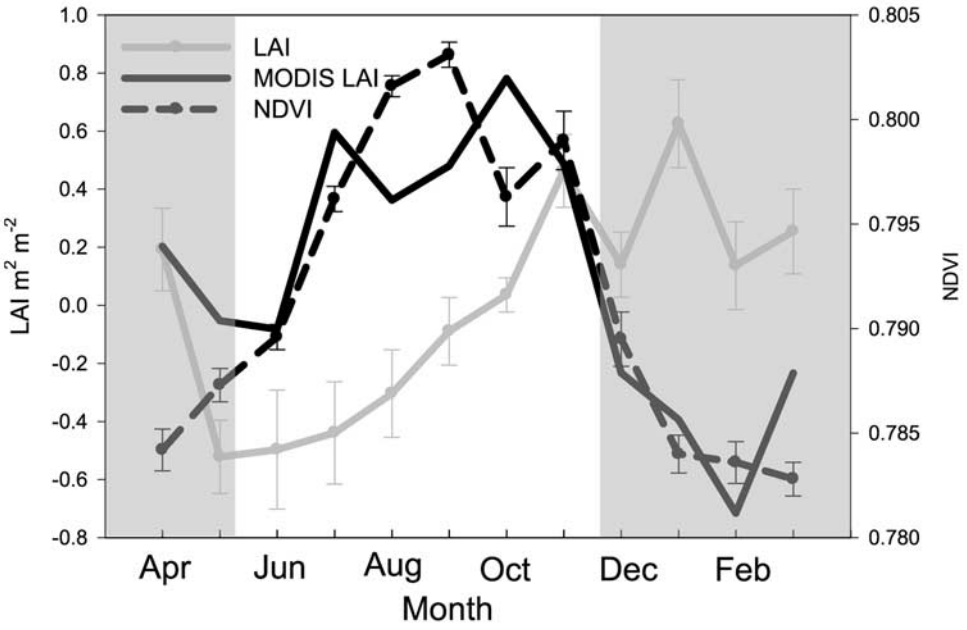


**Figure 4.** Monthly MODIS leaf area index (LAI; $m^2$ $m^{-2}$; MOD15 V004; solid black line connecting monthly averages across years) for the LBA-ECO km-83 site from 2000 to 2006. In situ normalized difference vegetation index (NDVI; dimensionless; black dashed line connecting monthly averages ± se, n varies from 85 to 394) at the km-83 tower during sunny periods from August 2001 to August 2003. In situ LAI ($m^2$ $m^{-2}$; gray line connecting monthly averages; ± se, n = 8) calculated from continuous observations of light intercepted by the canopy during sunny periods from August 2001 to March 2004. The annual means were removed from both LAI time series to better illustrate the seasonality. Shaded areas show the typical wet season.

positive from July to October, implying an increase in LAI during this period. The sum of litterfall and dLAI was calculated to determine the seasonal patterns of leaf flushing and production. Leaf production was comparatively low from November through June and much greater from July through October.

### 3.7. Leaf-Level Photosynthesis

[33] The rates of leaf gas exchange declined as leaves aged. For example, young *Tachigali mymercophyla* leaves had a photosynthetic capacity that was 27% greater than leaves that were one year old (Figure 6). Similarly, the rates of leaf photosynthesis by *Lecythis lurida,* which retained leaves for ~2 years, dropped by 46% from year 1 to year 2. Additional measurements on other species and at other nearby field sites, gave similar results [*Doughty et al.*, 2006; *Doughty and Goulden*, 2008]. Leaves that were at least one month old had higher rates of photosynthesis than older leaves; leaves required a month to mature and achieve peak photosynthesis. These results are consistent with previous observations showing that new leaves have higher photosynthetic rates under fixed environmental conditions than do older leaves [*Field and Mooney*, 1983; *Kitajima et al.*, 1997].

## 4. Discussion

### 4.1. How Does LAI Vary Seasonally?

[34] The in situ measurements of LAI and litterfall provide a quantitative picture of leaf phenology. Leaf production and leaf abscission were relatively low from December through April (Figure 5), a period that extended through most of the wet season (Figure 1). The low rates of leaf growth and abscission during this period resulted in a relatively high and constant LAI (Figure 4). Leaf abscission increased in May (Figure 5) when precipitation was still abundant (Figure 1). This increased abscission occurred in the absence of increased leaf production (Figure 5), which resulted in a reduced LAI (Figure 4). Leaf production accelerated in July through September, along with litterfall (Figure 5). The July through September period consisted of rapid leaf turnover (Figure 5), with many trees exchanging old leaves for new leaves. The LAI increased moderately during this period (Figure 4). Leaf abscission decreased abruptly in October (Figure 5), while production continued, which rapidly increased LAI (Figure 4).

[35] These observations of leaf phenology are consistent with those reported previously for tropical forests [*van Schaik et al.*, 1993]. Moreover, the observed seasonality is similar to that hypothesized for km-83 by *Goulden et al.* [2004]. The onset of leaf abscission in May occurred late in the wet season, during a period when precipitation was still frequent and the soil was wet [*Bruno et al.*, 2006]. Similarly, the accelerated leaf flushing from July through October occurred during the driest period of the year. The seasonal changes in leaf abscission and production were only indirectly related to the timing of rainfall [*van Schaik et al.*, 1993]. Leaf phenology at our site was not controlled by changing soil water availability but instead by factors such

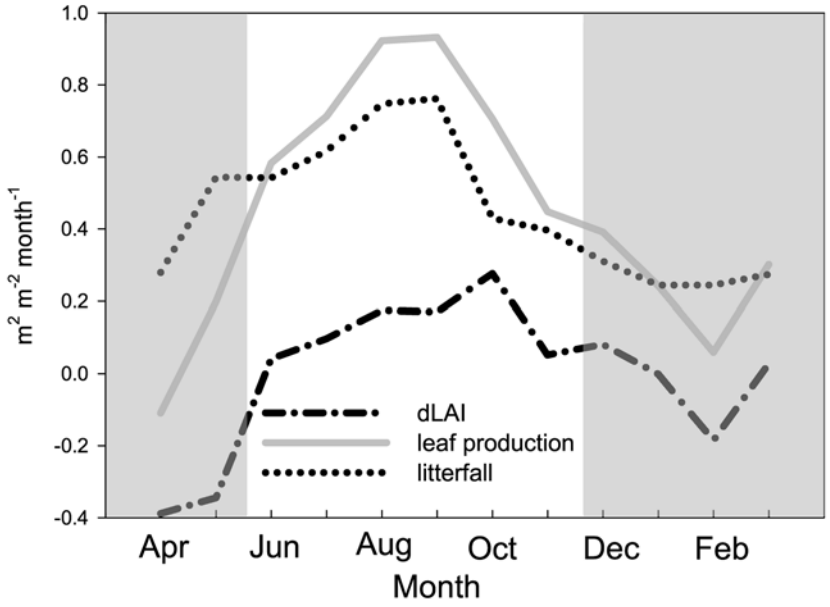


**Figure 5.** Leaf litterfall ($m^2$ $m^{-2}$ $month^{-1}$; dotted line connecting monthly values) during September 2000 and August 2001 from 20 litter baskets. Monthly change in LAI (dLAI; $m^2$ $m^{-2}$ $month^{-1}$; dot dash line connecting monthly values) during August 2001 to March 2004 calculated as the derivative of in situ LAI measurements (Figure 4). Leaf production ($m^2$ $m^{-2}$ $month^{-1}$; gray line connecting monthly values) calculated by adding the monthly litterfall and dLAI values. Shaded areas show the typical wet season.

as changing photoperiod [*Rivera et al.*, 2002], genetic control, or a complex interaction between the two.

### 4.2. Why Do the in Situ and MODIS-Based LAI Measurements Disagree?

[36] The seasonal changes in MODIS LAI at km-83 differed from the in situ measurements of LAI (Figure 4). Several considerations increase our confidence in the in situ LAI measurements. Our approach is simple, well established [*Fuchs et al.*, 1984; *Pierce and Running*, 1988; *Welles and Cohen*, 1996], and especially well suited for determining the relative LAI changes over a year [*Breda*, 2003; *Wang et al.*, 2004]. Sensitivity analyses confirmed that the seasonal cycle of LAI was not a result of our primary assumptions. Artifacts associated with seasonal changes in canopy geometry would be expected to cause trends that differ from those observed; a reduction in leaf exposure with drought would cause a decline in apparent LAI during the dry season, which is opposite the trend we observed. Similarly, artifacts associated with seasonal changes in incident radiation would be expected to cause transitions that coincide with the change of seasons, whereas the LAI transitions observed tended to occur in the middle of seasons. The increase in subcanopy light due to logging might have slightly affected the mean LAI measurements, but not the seasonal patterns. Finally, the seasonal patterns of LAI and leaf production were similar to the anecdotal observations of leaf growth we made during

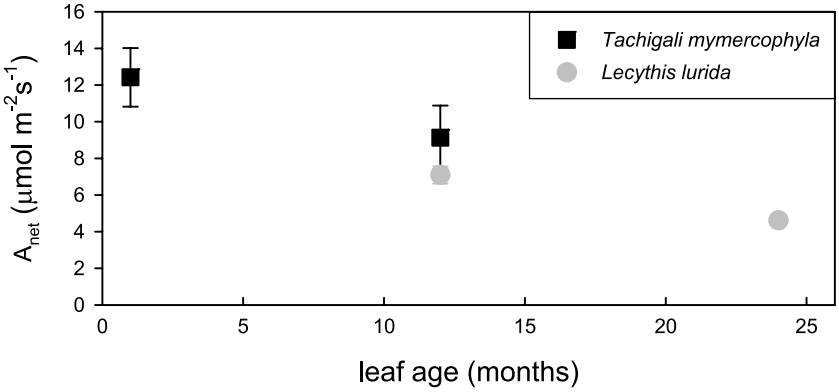


**Figure 6.** Leaf photosynthesis ($A_{net}$; $\mu$mol $CO_2$ $m^{-2}$ $s^{-1}$; averages ± se) by two canopy species (*Tachigali mymercophyla* (black squares; n = 6) and *Lecythis lurida* (gray circle; n = 15)) as a function of leaf age. All measurements were made during 2004 and 2005 at a PPFD of 1000 $\mu$mol $m^{-2}$ $s^{-1}$ and a chamber temperature of 30°C.

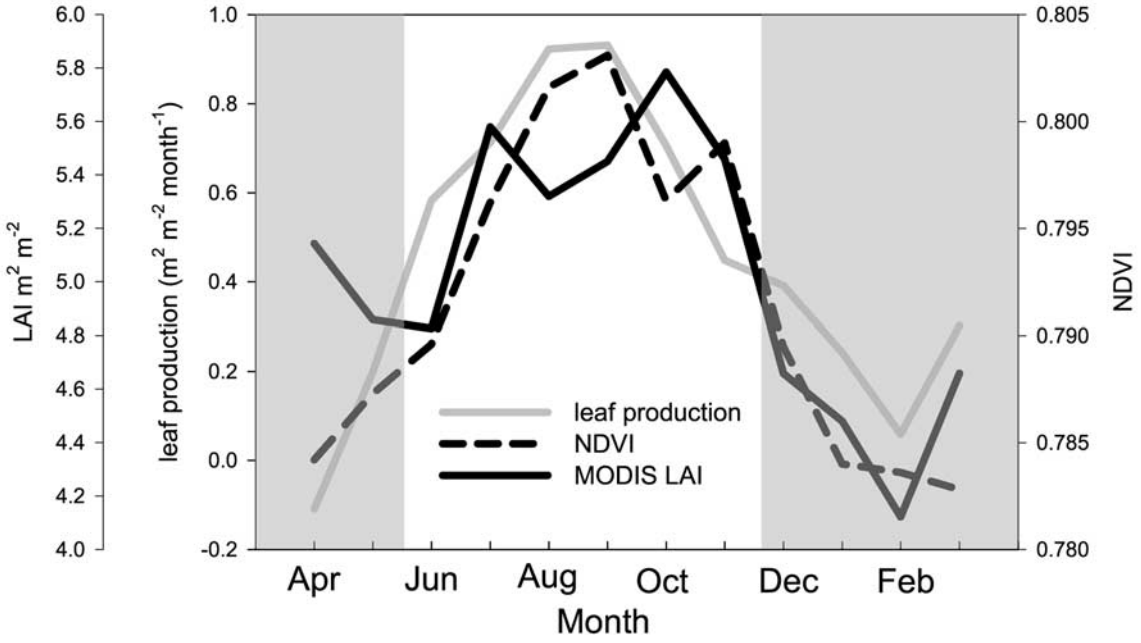


**Figure 7.** Monthly MODIS leaf area index (solid black line; see Figure 4 for details), leaf production (solid gray line; see Figure 5 for details), and in situ NDVI (black dashed line; see Figure 4 for details). Shaded areas show the typical wet season.

weekly visits to the site over several years, as well as observations in other tropical forests [*van Schaik et al.*, 1993].

[37] The MODIS LAI product for km-83 was not consistent with the suite of in situ observations. For example, the seasonal patterns of MODIS LAI diverged from the seasonal trends in canopy $CO_2$ exchange. MODIS LAI decreased from October to December to February (Figure 2) while the rates of light-saturated GEE were increasing (Figure 1). Perhaps most significantly, the MODIS LAI product indicated a large reduction in LAI in December (Figure 4). This decrease in LAI would be expected to result in a transient increase in litterfall. However, litterfall remained low during December (Figure 5), and we found no evidence, either direct or anecdotal, of an increase in leaf abscission at km-83 during this period. Previous studies have also noted discrepancies between the seasonal patterns of in situ measured and MODIS-derived LAI [*Wang et al.*, 2004; *Cohen et al.*, 2006].

[38] The MODIS LAI algorithm is based on the reflectance of red and NIR radiation [*Shabanov et al.*, 2005]. The July through November increases in in situ NDVI and MODIS LAI were a result of increased NIR reflectance (Figures 3 and 4). The NIR reflectance of canopies increases to a LAI of 4 to 5 $m^2m^{-2}$, at which point it saturates and becomes largely insensitive to incremental LAI change [cf. *Asner*, 1998]. The LAI at km-83 was always at least 5 to 6 $m^2$ $m^{-2}$, and we might expect the MODIS LAI algorithm would have difficulty detecting seasonal changes in LAI at this site.

[39] In fact, the MODIS LAI product was far better correlated at km-83 with the production of new leaves (Figure 7) than the absolute LAI (Figure 4). The rates of leaf flushing, the in situ NDVI, and the MODIS LAI were all increased from July through November and decreased from December through June. The MODIS LAI algorithm assumes the spectral reflectance of leaves remains constant [*Myneni et al.*, 2007], even though the NIR reflectance of tropical leaves has been shown to decrease markedly with time and the accumulation of leaf epiphylls [*Roberts et al.*, 1998]. We therefore suspect the dry season MODIS LAI increase at km-83 was actually a result of leaf flushing, and an increase in NIR reflectance by young leaves. Similarly, we suspect the December MODIS LAI decrease at km-83 was actually a result of leaf aging, increased epiphyll cover, and decreased NIR reflectance.

[40] We tested our hypothesis using a two-stream radiation transfer model [*Dickinson*, 1983] to combine the leaf flush and LAI data (Figures 4 and 5) with previously published observations of the change in leaf NIR absorption with leaf age [*Roberts et al.*, 1998]. We compared the observed seasonal patterns of whole canopy NIR albedo (Figure 3) with the seasonal patterns of albedo calculated in two ways: (1) assuming constant LAI and seasonally varying leaf age and NIR reflectance, and (2) assuming seasonally varying LAI and constant leaf NIR reflectance. The seasonal pattern of NIR absorption calculated assuming constant LAI and seasonally varying leaf NIR reflectance was qualitatively similar to that observed by tower measurements, though the amplitudes of seasonal variation differed by a factor of $\sim$3 (Figure 8). This discrepancy may reflect a difference in leaf properties or epiphyll concentrations between sites. The seasonal pattern of NIR absorption calculated assuming seasonally varying LAI and constant leaf-level NIR reflectance showed almost no variation, with an amplitude of seasonal variation that was two orders of magnitude less than observed (Figure 8). Leaf spectral changes played a far larger role in the seasonal cycle of whole-forest NIR reflectance than LAI, a pattern that is consistent with a saturation of NIR reflectance at high LAI.

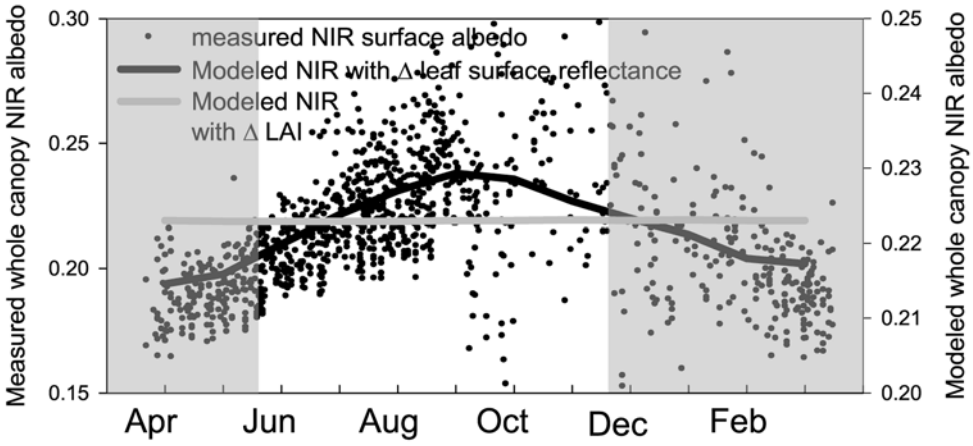


**Figure 8.** (small black circles) Whole-canopy Near Infrared (NIR) albedo (calculated by dividing reflected NIR by incident NIR) during sunny periods. (solid black line) Whole canopy NIR albedo calculated using a two stream radiation transfer model after accounting for the seasonal pattern of leaf reflectance due to the growth of epiphylls. (solid gray line) Whole canopy NIR albedo calculated after accounting for only the seasonal pattern of LAI. The modeled and observed data are scaled differently to improve clarity. Shaded areas show the typical wet season.

### 4.3. Why Does $CO_2$ Exchange Vary Seasonally?

[41] *Goulden et al.* [2004] hypothesized that seasonal changes in LAI at km-83 account for the seasonal patterns of $CO_2$ uptake. The observations of leaf phenology at km-83 supported the first element of Goulden et al.'s hypothesis; the LAI at km-83 was reduced during the late wet season and early dry season (Figure 4). However, the second element of Goulden et al.'s hypothesis, that these changes in LAI were sufficient to cause the observed changes in GEE, requires further testing. We developed three simple, observation-driven models of canopy gas exchange to investigate the causes of canopy gas exchange seasonality.

[42] The first model assumed that the seasonal shifts in canopy gas exchange were driven exclusively by seasonal

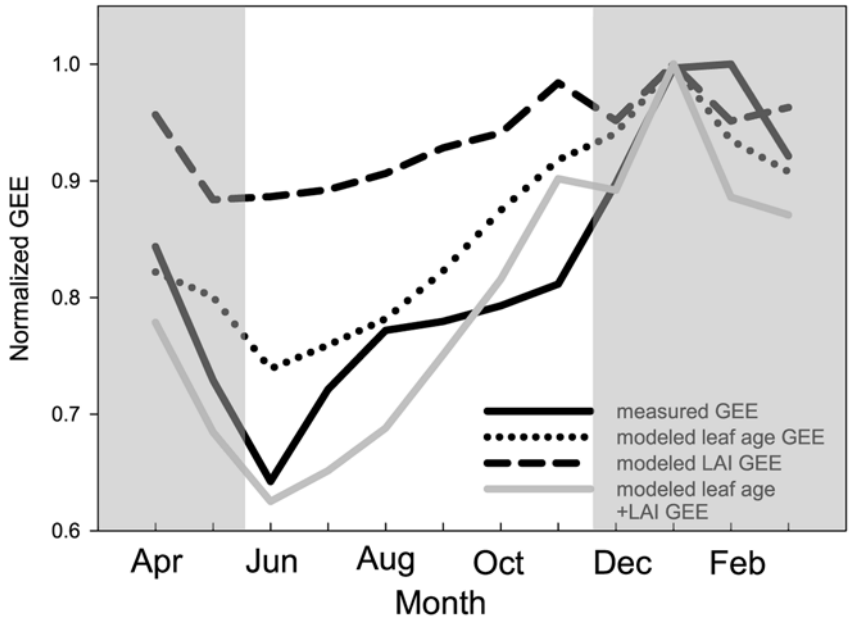


**Figure 9.** (solid black line) Observed light-saturated gross ecosystem exchange (GEE; see Figure 1 for details). (dashed line) GEE calculated using a model that assumed the seasonal shifts in canopy gas exchange were driven exclusively by seasonal changes in LAI. (dotted line) GEE calculated using a model that assumed the seasonal shifts in canopy gas exchange were driven exclusively by seasonal changes in leaf age and concomitant changes in leaf-level photosynthesis. GEE calculated combining the effect of seasonal changes in leaf age and LAI (solid gray line). Each curve was normalized to a value of 1.0 by the maximum monthly observation; the curves are dimensionless and a value of 0.7 corresponds to 70% of the maximum observed. Shaded areas show the typical wet season.

changes in LAI. This model showed that the seasonal patterns of LAI were insufficient to account for all of the observed changes in GEE (Figure 9). The seasonal amplitude of GEE caused by changing LAI was only 27% of that observed, as determined by linear regression. The forest's LAI was always at least 5 to 6 $m^2m^{-2}$. The canopy had sufficient leaves year-round to intercept nearly all of the incident radiation, and the seasonal changes in LAI did not result in a large change in the absolute amount of light intercepted by the canopy.

[43] The second model assumed that seasonal shifts in canopy gas exchange were driven exclusively by seasonal changes in leaf age and leaf-level photosynthesis. This model did a better job of accounting for the observed changes in GEE (Figure 9). The increase in light-saturated GEE from August through January (Figure 1) appears to result mainly from the flushing of leaves (Figure 5) and a shift to younger leaves, which have higher rates of gas exchange (Figure 6). However, the observed seasonal changes in normalized GEE were greater than could be accounted for by leaf aging alone (Figure 9); the seasonal amplitude of normalized GEE caused by changing leaf age was only 67% of that observed.

[44] The third model assumed that seasonal shifts in canopy gas exchange were driven by both seasonal changes in LAI and leaf-level photosynthesis. This model did the best job of reproducing the seasonal cycle of light-saturated GEE (Figure 9). The seasonal amplitude of normalized GEE caused by the combination of changing LAI and leaf age was 95% of that observed. We therefore reject the second element of Goulden et al.'s hypothesis, and conclude that the seasonal changes in GEE at km-83 are related to both the effect of leaf aging and LAI, with leaf aging playing the dominant role.

[45] **Acknowledgments.** We thank Helber Freitas, Michela Figueira, Augusto Maia, and Albert de Sousa for field help; Scott Miller and Humberto da Rocha for help with the tower measurements; UFPA in Santarém and Belem for help identifying species; Susan Trumbore for comments; and the LBA-ECO Santarém field office for support. This work was funded by NASA as a component of LBA-ECO and by NASA's Earth System Science fellowship.

## References

Asner, G. P. (1998), Biophysical and biochemical sources of variability in canopy reflectance, *Remote Sens. Environ.*, *64*(3), 234–253.

Asner, G. P., D. Nepstad, G. Cardinot, and D. Ray (2004), Drought stress and carbon uptake in an Amazon forest measured with spaceborne imaging spectroscopy, *Proc. Natl. Acad. Sci. U. S. A.*, *101*(16), 6039–6044.

Baldocchi, D. D. (2003), Assessing the eddy covariance technique for evaluating carbon dioxide exchange rates of ecosystems: Past, present and future, *Global Change Biol.*, *9*(4), 479–492.

Bonan, G. B. (2002), *Ecological Climatology*, 678 pp., Cambridge Univ. Press, New York.

Breda, N. J. J. (2003), Ground-based measurements of leaf area index: A review of methods, instruments and current controversies, *J. Exp. Bot.*, *54*(392), 2403–2417.

Bruno, R. D., H. R. da Rocha, H. C. de Freitas, M. L. Goulden, and S. D. Miller (2006), Soil moisture dynamics in an eastern Amazonian tropical forest, *Hydrol. Process.*, *20*(12), 2477–2489.

Carswell, F. E., et al. (2002), Seasonality in $CO_2$ and $H_2O$ flux at an eastern Amazonian rain forest, *J. Geophys. Res.*, *107*(D20), 8076, doi:10.1029/2000JD000284.

Cohen, W. B., T. K. Maiersperger, D. P. Turner, W. D. Ritts, D. Pflugmacher, R. E. Kennedy, A. Kirschbaum, S. W. Running, M. Costa, and S. T. Gower (2006), MODIS land cover and LAI collection 4 product quality across nine sites in the Western Hemisphere, *IEEE Trans. Geosci. Remote Sens.*, *44*(7), 1843–1857.

da Rocha, H. R., M. L. Goulden, S. D. Miller, M. C. Menton, L. D. V. O. Pinto, H. C. de Freitas, and A. M. E. S. Figueira (2004), Seasonality of water and heat fluxes over a tropical forest in eastern Amazonia, *Ecol. Appl.*, *14*(4), S22–S32.

Dickinson, R. E. (1983), Land surface processes and climate surface albedos and energy-balance, *Adv. Geophys.*, *25*, 305–353.

Doughty, C. E., and M. L. Goulden (2008), Are tropical forests near a high temperature threshold?, *J. Geophys. Res.*, doi:10.1029/2007JG000632, in press.

Doughty, C. E., M. L. Goulden, S. D. Miller, and H. R. da Rocha (2006), Circadian rhythms constrain leaf and canopy gas exchange in an Amazonian forest, *Geophys. Res. Lett.*, *33*, L15404, doi:10.1029/2006GL026750.

Field, C., and H. A. Mooney (1983), Leaf age and seasonal effects on light, water, and nitrogen use efficiency in a California shrub, *Oecologia*, *56*(2–3), 348–355.

Figueira, A. M. S., S. D. Miller, A. D. C. de Sousa, M. C. Menton, A. R. Maia, H. R. da Rocha, and M. L. Goulden (2008), Effects of selective logging on tropical forest tree growth, *J. Geophys. Res.*, doi:10.1029/2007JG000577, in press.

Fuchs, M., G. Asrar, E. T. Kanemasu, and L. E. Hipps (1984), Leaf-area estimates from measurements of photosynthetically active radiation in wheat canopies, *Agric. For. Meteorol.*, *32*(1), 13–22.

Goulden, M. L., S. D. Miller, H. R. da Rocha, M. C. Menton, H. C. de Freitas, A. M. E. S. Figueira, and C. A. D. de Sousa (2004), Diel and seasonal patterns of tropical forest $CO_2$ exchange, *Ecol. Appl.*, *14*(4), S42–S54.

Goulden, M. L., S. D. Miller, and H. R. da Rocha (2006), Nocturnal cold air drainage and pooling in a tropical forest, *J. Geophys. Res.*, *111*, D08S04, doi:10.1029/2005JD006037.

Huemmrich, K. F., T. A. Black, P. G. Jarvis, J. H. McCaughey, and F. G. Hall (1999), High temporal resolution NDVI phenology from micrometeorological radiation sensors, *J. Geophys. Res.*, *104*(D22), 27,935–27,944.

Huete, A. R., K. Didan, Y. E. Shimabukuro, P. Ratana, S. R. Saleska, L. R. Hutyra, W. Z. Yang, R. R. Nemani, and R. Myneni (2006), Amazon rainforests green-up with sunlight in dry season, *Geophys. Res. Lett.*, *33*, L06405, doi:10.1029/2005GL025583.

Kitajima, K., S. S. Mulkey, and S. J. Wright (1997), Decline of photosynthetic capacity with leaf age in relation to leaf longevities for five tropical canopy tree species, *Am. J. Bot.*, *84*(5), 702–708.

Malhi, Y., A. D. Nobre, J. Grace, B. Kruijt, M. G. P. Pereira, A. Culf, and S. Scott (1998), Carbon dioxide transfer over a Central Amazonian rain forest, *J. Geophys. Res.*, *103*(D24), 31,593–31,612.

Miller, S. D., M. L. Goulden, M. C. Menton, H. R. da Rocha, H. C. de Freitas, A. M. E. S. Figueira, and C. A. D. de Sousa (2004), Biometric and micrometeorological measurements of tropical forest carbon balance, *Ecol. Appl.*, *14*(4), S114–S126.

Miller, S. D., M. L. Goulden, and H. R. da Rocha (2007), The effect of canopy gaps on subcanopy ventilation and scalar fluxes in a tropical forest, *Agric. For. Meteorol.*, *142*(1), 25–34.

Myneni, R. B., et al. (2007), Large seasonal swings in leaf area of Amazon rainforests, *Proc. Natl. Acad. Sci. U. S. A.*, *104*(12), 4820–4823.

Nepstad, D. C., C. R. Decarvalho, E. A. Davidson, P. H. Jipp, P. A. Lefebvre, G. H. Negreiros, E. D. Dasilva, T. A. Stone, S. E. Trumbore, and S. Vieira (1994), The role of deep roots in the hydrological and carbon cycles of Amazonian forests and pastures, *Nature*, *372*(6507), 666–669.

Nepstad, D. C., et al. (2002), The effects of partial throughfall exclusion on canopy processes, aboveground production, and biogeochemistry of an Amazon forest, *J. Geophys. Res.*, *107*(D20), 8085, doi:10.1029/2001JD000360.

Pierce, L. L., and S. W. Running (1988), Rapid estimation of coniferous forest leaf-area index using a portable integrating radiometer, *Ecology*, *69*(6), 1762–1767.

Rivera, G., S. Elliott, L. S. Caldas, G. Nicolossi, V. T. R. Coradin, and R. Borchert (2002), Increasing day-length induces spring flushing of tropical dry forest trees in the absence of rain, *Trees Structure Function*, *16*(7), 445–456.

Roberts, D. A., B. W. Nelson, J. B. Adams, and F. Palmer (1998), Spectral changes with leaf aging in Amazon caatinga, *Trees Structure Function*, *12*(6), 315–325.

Saleska, S. R., et al. (2003), Carbon in amazon forests: Unexpected seasonal fluxes and disturbance-induced losses, *Science*, *302*(5650), 1554–1557.

Shabanov, N. V., et al. (2005), Analysis and optimization of the MODIS leaf area index algorithm retrievals over broadleaf forests, *IEEE Trans. Geosci. Remote Sens.*, *43*(8), 1855–1865.

van Schaik, C. P., J. W. Terborgh, and S. J. Wright (1993), The phenology of tropical forests - Adaptive significance and consequences for primary consumers, *Annu. Rev. Ecol. Syst.*, *24*, 353–377.

Wang, Q., J. Tenhunen, A. Granier, M. Reichstein, O. Bouriaud, D. Nguyen, and N. Breda (2004), Long-term variations in leaf area index

and light extinction in a Fagus sylvatica stand as estimated from global radiation profiles, *Theor. Appl. Climatol.*, *79*, 225–238.

Welles, J. M., and S. Cohen (1996), Canopy structure measurement by gap fraction analysis using commercial instrumentation, *J. Exp. Bot.*, *47*(302), 1335–1342.

Williams, M., Y. Malhi, A. D. Nobre, E. B. Rastetter, J. Grace, and M. G. P. Pereira (1998), Seasonal variation in net carbon exchange and evapotranspiration in a Brazilian rain forest: A modeling analysis, *Plant Cell Environ.*, *21*(10), 953–968.

Wofsy, S. C., M. L. Goulden, J. W. Munger, S. M. Fan, P. S. Bakwin, B. C. Daube, S. L. Bassow, and F. A. Bazzaz (1993), Net exchange of $CO_2$ in a midlatitude forest, *Science*, *260*(5112), 1314–1317.

Xiao, X. M., Q. Y. Zhang, S. Saleska, L. Hutyra, P. De Camargo, S. Wofsy, S. Frolking, S. Boles, M. Keller, and B. Moore (2005), Satellite-based modeling of gross primary production in a seasonally moist tropical evergreen forest, *Remote Sens. Environ.*, *94*(1), 105–122.

C. E. Doughty and M. L. Goulden, Department of Earth System Science, University of California, Irvine, CA 92697-3100, USA. (cdoughty@stanford.edu)